

Progressive structural and biomechanical changes in elastin degraded aorta

Ming-Jay Chow · Jarred R. Mondonedo ·
Victor M. Johnson · Yanhang Zhang

Received: 4 August 2011 / Accepted: 1 May 2012 / Published online: 24 May 2012
© Springer-Verlag 2012

Abstract Aortic aneurysm is an important clinical condition characterized by common structural changes such as the degradation of elastin, loss of smooth muscle cells, and increased deposition of fibrillary collagen. With the goal of investigating the relationship between the mechanical behavior and the structural/biochemical composition of an artery, this study used a simple chemical degradation model of aneurysm and investigated the progressive changes in mechanical properties. Porcine thoracic aortas were digested in a mild solution of purified elastase (5 U/mL) for 6, 12, 24, 48, and 96 h. Initial size measurements show that disruption of the elastin structure leads to increased artery dilation in the absence of periodic loading. The mechanical properties of the digested arteries, measured with a biaxial tensile testing device, progress through four distinct stages termed (1) initial-softening, (2) elastomer-like, (3) extensible-but-stiff, and (4) collagen-scaffold-like. While stages 1, 3, and

4 are expected as a result of elastin degradation, the S-shaped stress versus strain behavior of the aorta resulting from enzyme digestion has not been reported previously. Our results suggest that gradual changes in the structure of elastin in the artery can lead to a progression through different mechanical properties and thus reveal the potential existence of an important transition stage that could contribute to artery dilation during aneurysm formation.

Keywords Elastin · Collagen · Aneurysm · Elastic instability · Biaxial tension · Degradation · Elastase · Elastomer

1 Introduction

Arteries remodel as a result of changes in blood flow, pressure, and other chemical factors (Martinez-Lemus et al. 2008; Pistea et al. 2005) and aneurysms are formed when a section of the arterial tissue becomes permanently distended. Abdominal aortic aneurysms (AAA) are an important clinical condition where ~150,000 new cases are diagnosed yearly with a mortality rate of 90% if rupture occurs (Vorp and Vande Geest 2005). Because of the high mortality rate of rupture, it is desirable to be able to predict when a patient should have surgery to repair the dilated tissue. Current clinical practices involve measuring the expansion rate and diameter of the artery. Other parameters such as wall stiffness and peak wall stress may offer better predictions as to when an aneurysm will fail and thus provide for better patient care (Vorp and Vande Geest 2005). In order to estimate the material properties of the aneurysm wall, understanding the relationship between artery structure and function is necessary.

Generally, arteries exhibit anisotropic and hyperelastic stress versus strain curves where the majority of the

M.-J. Chow
Department of Mechanical Engineering, Boston University,
110 Cummington Street, Boston, MA 02215, USA

J. R. Mondonedo
Department of Biomedical Engineering, Boston University,
110 Cummington Street, Boston, MA 02215, USA

V. M. Johnson
Department of Anesthesiology, Perioperative and Pain Medicine,
Children's Hospital Boston, Harvard Medical School, Boston,
MA 02115, USA

Y. Zhang (✉)
Department of Mechanical Engineering, Department of Biomedical
Engineering, Boston University, 110 Cummington Street, Boston,
MA 02215, USA
e-mail: yanhang@bu.edu

passive mechanical behavior is due to the collagen and elastin extracellular matrix (ECM) (Dahl et al. 2007; Dobrin 1978; Fonck et al. 2007). The initial softer region of the stress versus strain curve has generally been attributed to the elastin fibers supporting the load, whereas the stiffened region is due to collagen fiber recruitment and collagen bearing the load (Cox 1978). Normal artery behavior between diastole and systole encompasses both the elastin-supported and collagen-supported regions (Valdez-Jasso et al. 2011). Previously, studies have found compositional and mechanical differences between aneurysm tissue and healthy tissue. Common structural changes in aneurysm tissue include an early loss of elastin and smooth muscle cells followed by an increase in fibrillary collagen. For example, a 90 % reduction in elastin and indicators of excess aged collagen/improper new collagen synthesis are reported in AAA specimens compared to non-aneurysmal abdominal tissue (Carmo et al. 2002). It has also been shown that there are significant changes in the media layer including a fragmentation of the elastic laminae and fibers (Lakatta et al. 1987). Regarding the mechanical properties, human aortic aneurysm tissue shows increased elastic modulus and anisotropy compared to healthy tissue (Matsumoto et al. 2009; Vande Geest et al. 2006).

Because of the limited access to human aneurysm tissue, chemical degradation methods have been used to create models for aortic aneurysm. Elastase digestion causes the elastin network to be disrupted in a manner similar to what occurs in the formation of an aneurysm (Fonck et al. 2007). Use of solutions such as calcium chloride or combinations of calcium chloride/elastase more closely approximate aneurysm formation by initiating inflammatory responses such as calcium deposition and smooth muscle injury (Tanaka et al. 2009; Gertz et al. 1988). The chemical models of aneurysm have been applied both *in vitro* and *in vivo*. *In vitro* methods generally include harvesting arteries and subjecting them to an enzymatic treatment by leaving arteries in a solution bath or through local topical application (Miskolczi et al. 1998). More complicated *in vivo* animal models involve surgically exposing an artery and delivering the chemical/enzyme solution either perivascularly (Isenburg et al. 2007) or by temporarily blocking an artery and delivering the intraluminal solution (Kallmes et al. 2002).

In the present study, we use *in vitro* mild elastase solutions to create gradual structural changes in the artery structure. Elastin and collagen assays quantify biochemical changes in the ECM and Movat's pentachrome stain reveal other structural changes not captured by the assays. Biaxial tensile testing is used to characterize the mechanical behavior of arteries, so we can relate the progressive changes in the mechanical properties of arteries with the gradual differences in microstructure and ECM components.

2 Materials and methods

2.1 Tissue preparation and chemical degradation

Porcine thoracic aortas were obtained from 12–24 month old pigs (160–200 lbs in weight) from a local abattoir and cleaned of loose connective/fatty tissue. Approximately, 1.5 ~ 2 cm sized square samples were cut, so that one edge was parallel to the longitudinal direction and the other edge was parallel to the circumferential direction of the artery. The thickness of each sample was taken at several locations with a pocket dial thickness gauge, and measurements were averaged. Samples of similar thicknesses were placed in a phosphate-buffered saline (1 × PBS) solution at 4 °C before further processing. A 5 U/mL ultra-pure elastase solution (MP Biomedicals, LLC, OH) was used to gradually degrade tissues at 37 °C with gentle stirring similar to the procedure detailed by Lu et al. (2004). A total of 60 samples were divided evenly into five time groups (6, 12, 24, 48, and 96 h, $n = 12$ at each of the five time points) to assess mechanical and structural changes after various digestion times. All samples were mechanically tested at the fresh condition ($n = 60$) within 24 h of tissue harvesting. After a period of digestion, samples were rinsed in deionized water and the post-digestion mechanical testing was performed.

2.2 Mechanical testing

A biaxial tensile testing device was used in this study to characterize the mechanical behavior of aortic tissue following protocols described previously (Grashow et al. 2006; Zou and Zhang 2009). Briefly, four carbon marker dots were applied on the tissue so that when tension was applied, the resulting stretch could be measured by tracking the position of the marker dots using a CCD camera with a refresh rate of 7–8 Hz. Elastase-treated samples are more porous and fragile. In order to reach physiologic meaningful stresses and limit damage to the tissue (Szczyzny et al. 2012), sandpaper tabs were attached to the top and bottom faces along the edges of the tissue samples with cyanoacrylate glue (Elmer's Products, OH). Sutures were then looped through the sandpaper fold and connected to the linear positioners. A tension control protocol was implemented using a Labview program (Sacks 1999). For all mechanical tests, a small preload of 2 ± 0.050 N/m was applied in order to straighten the sutures connecting the tissue to the device. Initially, the samples were put through a series of eight preconditioning cycles in which they were loaded in both directions to 30 N/m for all tissues. Following preconditioning, eight cycles of equi-biaxial tension were applied to capture the anisotropic mechanical behavior. Data used for the analysis came from the eighth cycle when the stress versus strain curves had become stable. Fresh tests generally exceeded 120 kPa and tests after

digestion had maximum stresses above 100 kPa. For consistency, 100 kPa was chosen as the maximum stress when comparing the results from both fresh and post-digestion tests.

Cauchy stresses were calculated based on plane stress and incompressibility assumptions (Humphrey et al. 2009):

$$\sigma_1 = \frac{F_1 \lambda_1}{L_{2o} t}, \quad \sigma_2 = \frac{F_2 \lambda_2}{L_{1o} t} \quad (1)$$

In Eq. (1), σ is the Cauchy stress, F is the applied load, λ is the stretch, L_o is the initial length, and t is the thickness of the tissue. The subscripts 1 and 2 correspond to the longitudinal and circumferential directions of the tissue, respectively. Cauchy stress versus Green strain was plotted to describe the mechanical response. Green strain E is calculated as (Holzapfel 2000):

$$E_i = \frac{1}{2} (\lambda_i^2 - 1) \quad (2)$$

where λ is the stretch and $i = 1, 2$.

2.3 Elastin and collagen assays

After mechanical testing, small pieces (approximately 1×5 mm) were cut from each of the fresh and digested tissues for elastin and collagen assays. Elastin content was measured using a Fastin elastin assay kit (Biocolor, www.biocolor.co.uk). The elastin assays measured soluble tropoelastins and insoluble elastin that was solubilized into α -elastin polypeptides following manufacturer's protocols. The optical density was measured at 513 nm using the microplate reader. Elastin content was expressed as μg of elastin/mg of wet tissue weight. The amount of soluble and insoluble collagen was determined following the extraction procedures described in detail by Reddy (2004). After isolating the volumes of different types of collagen, the samples were analyzed using a Sircol collagen assay kit (Biocolor, www.biocolor.co.uk) following manufacturer's instructions. The Sircol collagen kit used a quantitative dye-binding method and absorbance was measured using a SpectraMax M5 plate reader (Molecular Devices) at a 540 nm wavelength. Collagen content was expressed as μg of collagen/mg of wet tissue weight.

2.4 Histology studies

After mechanical testing, randomly selected samples from each group were fixed in 10% formaldehyde (Fisher Scientific) for histological studies. A cross-section was cut along the circumferential direction, and the Movat's pentachrome stain was used to identify changes in the arterial structure. The Movat's stain allowed for identification of collagen fibers (yellow), smooth muscle cells (red), ground substance (blue), and nuclei/elastic fibers (purple to black) (Taylor et al. 1999; Arbustini et al. 2002).

2.5 Statistical analysis

Experimental data were summarized with mean \pm SD. Values of elastin and soluble, insoluble, total, and cross-linked collagen in fresh arteries were compared to data gathered after elastase digestion using generalized estimating equations taking into account the repeated measures (Liang and Zeger 1986). Comparisons of the strains in both the longitudinal and circumferential directions were made between fresh and digested arteries in the same manner as described above. A two-tailed $P < 0.05$ was considered statistically significant with post hoc test using the Bonferroni procedure to adjust for multiple comparisons. Statistical analysis was performed using the SPSS statistical package (version 19.0, SPSS Inc./IBM, Chicago, IL).

3 Results

As a result of the digestion with the elastase solution, the artery samples transition from an opaque solid material to a translucent gel-like structure. The fresh artery thickness varied from 0.84 to 1.95 mm (mean = 1.32 ± 0.21 mm). The thicknesses of the digested arteries are not reported here due to the uncertainty in measurements due to the formation of the gel-like structure. In both the longitudinal and circumferential directions (Fig. 1a, b), there is a significant increase in the side length of the artery samples after digestion ($P < 0.001$). This increase in size occurs purely as a result of the removal of elastin.

Figure 2 shows the elastin content of the arteries decreases with increased time of enzyme treatment ($P < 0.001$). In Fig. 3, the total collagen is calculated by adding the soluble collagen with the insoluble collagen. The percent of cross-linked collagen is determined by dividing the amount of insoluble collagen by the total amount of collagen (Reddy 2004). Collagen assays show a significant increase in total collagen, insoluble collagen, and collagen cross-linking ($P < 0.001$) in all cases except in the total collagen after 6 h of digestion ($P = 0.059$). The amounts of soluble collagen are not significantly different between fresh and digested tissues ($P > 0.148$) except after 48 h of digestion ($P = 0.006$).

The Movat's pentachrome stains reveal some common characteristics of aneurysm tissue. The elastase digestion creates regions of loose/coiled elastin fibers (Fig. 4b) and fragmented elastin fibers (Fig. 4b, d). Loss of smooth muscle cells is evidenced by the disappearance of red-colored cells and dark blackish nuclei within the remaining collagen layers (Fig. 4b, c, d, e, f) and also between elastic fibers in Fig. 4d. Note that elastase does not digest elastin through the thickness in an even manner, but rather begins at the exterior surfaces and progresses inwardly. The center of the media is relatively preserved through the 12 h time point (Fig. 4c) and

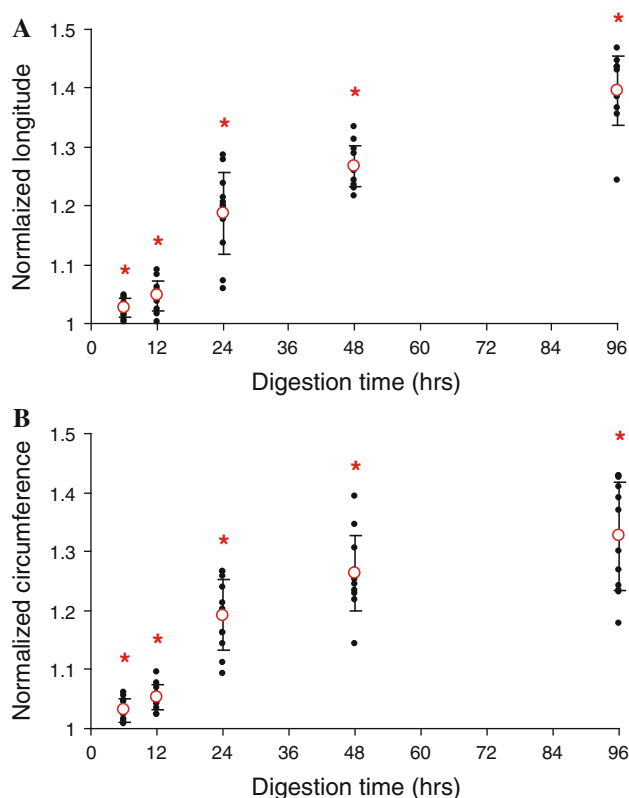


Fig. 1 Changes in the size of the *longitudinal* (a) and *circumferential* (b) directions of the tissue after treating with elastase for 6, 12, 24, 48, and 96 h ($n = 12$). The lengths post-digestion were normalized to the fresh tissue measurements. * $P < 0.05$

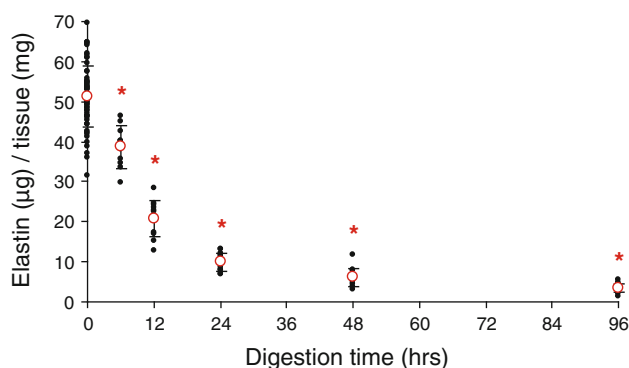


Fig. 2 Elastin content, expressed as ug of elastin per mg of wet tissue weight, at fresh conditions (0h, $n = 60$) and after treating with elastase for 6, 12, 24, 48, and 96 h ($n = 12$). * $P < 0.05$

layers of elastin still remain in the very center after 24 h of digestion (Fig. 4d). The remaining tissue after 48 and 96 h of digestion is primarily collagen and contains minimal elastin (Fig. 4e, f).

Figure 5 shows the averaged Cauchy stress versus Green strain curves from the biaxial tensile tests. The fresh arteries (Fig. 5a) display anisotropic and hyperelastic behavior with the circumferential being stiffer than the longitudinal

direction. After 6 h of digestion, the initial slopes of the curves are mildly reduced, but the overall behavior still has the anisotropic hyperelastic properties (Fig. 5b). After 12 h of digestion, an elastomer-like behavior is seen in the longitudinal direction as the stress versus strain curve loses the J-shape and becomes more S-shaped (Fig. 5c, the S-shaped curve is not very prominent in the averaged data, and a clearer example of the S-shape behavior from a single artery is shown later in Fig. 7). At 24 h of digestion, the arteries have a pronounced J-shape curve with a very low initial slope, extended toe region, and prominent strain stiffening at higher strains (Fig. 5d). Finally, after 48 and 96 h of digestion, the stress versus strain curves lose the initial toe region and are very stiff shortly after the onset of loading (Fig. 5e, f).

Figure 6 shows representative Cauchy stress versus Green strain curves and the progression of the mechanical properties through four major stages: initial-softening (IS), elastomer-like (EL), extensible-but-stiff (ES), and collagen-scaffold (CS) behavior, note only the longitudinal direction is shown. Table 1 shows the changes in the frequencies of normal/fresh (F), IS, EL, ES, and CS behavior with the elastase digestion periods. Note that after 6 h of digestion, the Cauchy stress versus Green strain behavior in the circumferential direction was almost unchanged for six samples and was counted as “fresh” behavior. The longitudinal strains of the digested tissue show statistically significant differences from strains of fresh tissue in the 6, 12, 48, and 96 h conditions ($P < 0.001$) but not in the 24 h condition ($P = 1.0$). For circumferential direction, there are statistically significant differences in the strains at the 12 ($P = 0.001$), 48 ($P < 0.001$), and 96 h ($P < 0.001$) conditions, but the 6 and 24 h digestions do not have significant differences from the fresh tissue ($P = 0.08$ and $P = 1.0$, respectively). Our mechanical results show the arteries have very different mechanical behavior depending on the amount of elastin digestion, which will be discussed later.

4 Discussion

In this study, arteries are treated with mild elastase solutions for five different durations to capture the progression of changes in mechanical properties. Our measurements show an increase in size of the arteries in both the longitudinal and circumferential directions following elastin digestion (Fig. 1). Previous experimental studies of arteries in dogs have also reported vessel dilation with elastase treatments (Dobrin and Canfield 1984), and artery dilation is a characteristic of aneurysms in general (Humphrey and Taylor 2008). It has been suggested that aneurysms may form due to cyclic loading that progressively weakens an artery that initially had structural damage (Gasser et al. 2008). Here, we show that the dimensions of arteries increase with elastin degradation

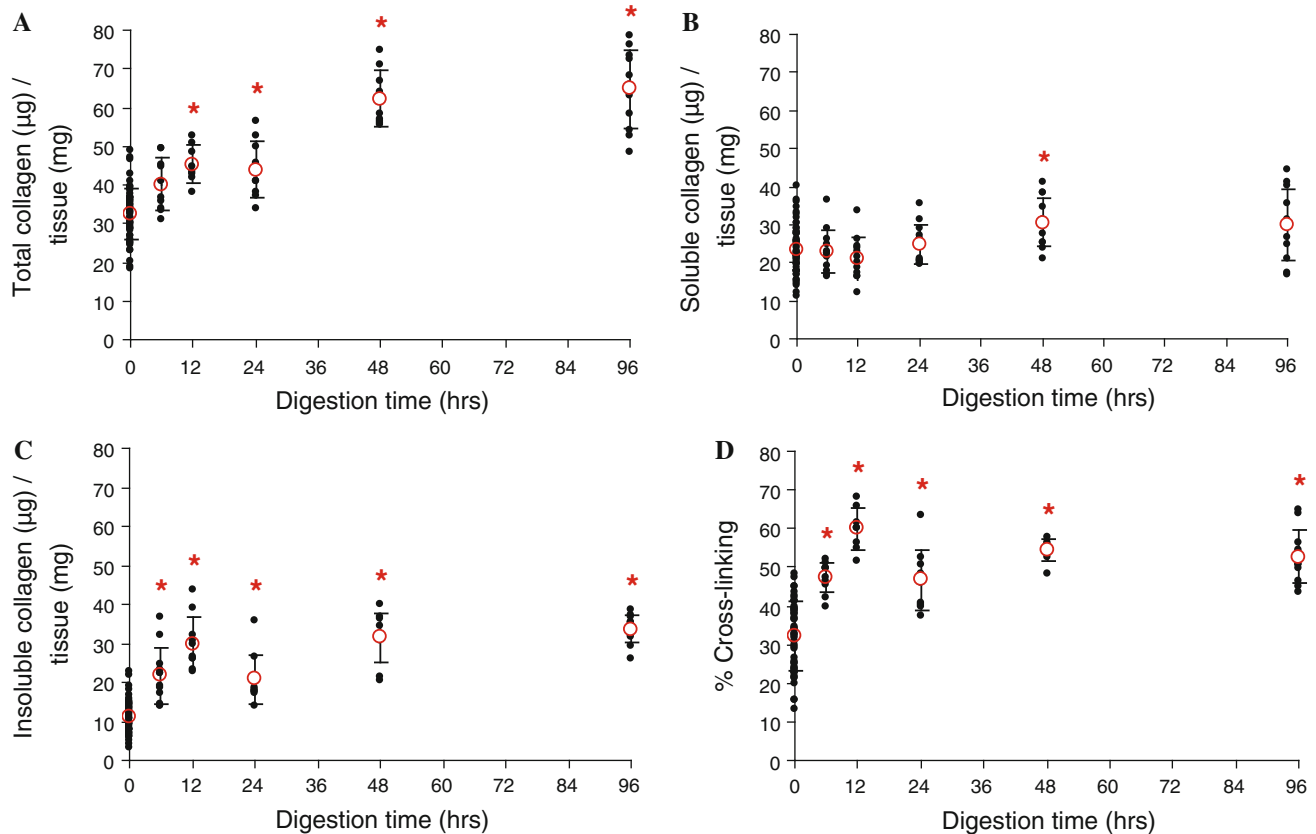


Fig. 3 Total (a), soluble (b), and insoluble (c) collagen, expressed as μg of collagen per mg of wet tissue weight, at fresh conditions (0h, $n = 60$) and after treating with elastase for 6, 12, 24, 48, and 96 h ($n = 12$). The percent of cross-linked collagen is also presented (d). * $P < 0.05$

prior to any preconditioning or loading. This indicates that the structural damage caused by removing elastin is enough to create artery dilation before pulsatile blood flow loading would further expand the structure.

Decreased elastin content in the media as well as the disruption and fragmentation of the elastic lamellae are common characteristics of aneurysms (Guo et al. 2011; Hellenenthal et al. 2009; Stanley et al. 1975). The decrease in elastin content with increased digestion time (Fig. 2) is further confirmed by the Movat's pentachrome stains of the artery cross-sections (Fig. 4). The histology slides also display other characteristics of aneurysm tissue such as loss of smooth muscle cells, which has been previously reported to occur in thoracic aortic aneurysm (Guo et al. 2011). Other characteristics of aneurysm including excess deposition of collagen, medial neovascularization, and inflammatory cell infiltration (Hellenenthal et al. 2009; Stanley et al. 1975) are not present in the current in vitro study.

During the formation of an aneurysm, there is generally an increase in the amount of collagen and collagen cross-linking in the artery (Humphrey and Taylor 2008) that has been attributed as a response of the body to compensate for the loss of elastin (Lasheras 2007). Our collagen

assay results also showed an increase in total collagen content and collagen cross-linking after the elastase treatment (Fig. 3a, d); however, this clearly is not due to arterial remodeling. The increase in collagen cross-linking is attributed to the increase in insoluble collagen (Fig. 3c) in this study. Our method of measuring insoluble collagen in the tissue involves denaturing covalently cross-linked collagen into gelatin for measurement with the Sircol collagen assay kit (Reddy 2004). As the artery is subjected to the elastase treatment, the process of removing elastin can also loosen/weaken the cross-linked collagen network. This would make the collagen network more susceptible to the denaturing process and thus the amounts of extracted insoluble collagen are higher.

The anisotropic and hyperelastic behavior of aortic tissue has been well documented and corresponds to the results from the fresh artery tests. Destruction of the elastin network leads to decreased stiffness in arteries (Lacolley et al. 2002), and this corresponds with our results where the loss of elastin causes the decreased slope and is characteristic of the first shift in mechanical behavior called the initial-softening phase.

The second stage that the artery behavior transitions to is termed elastomer-like because the stress versus strain curves

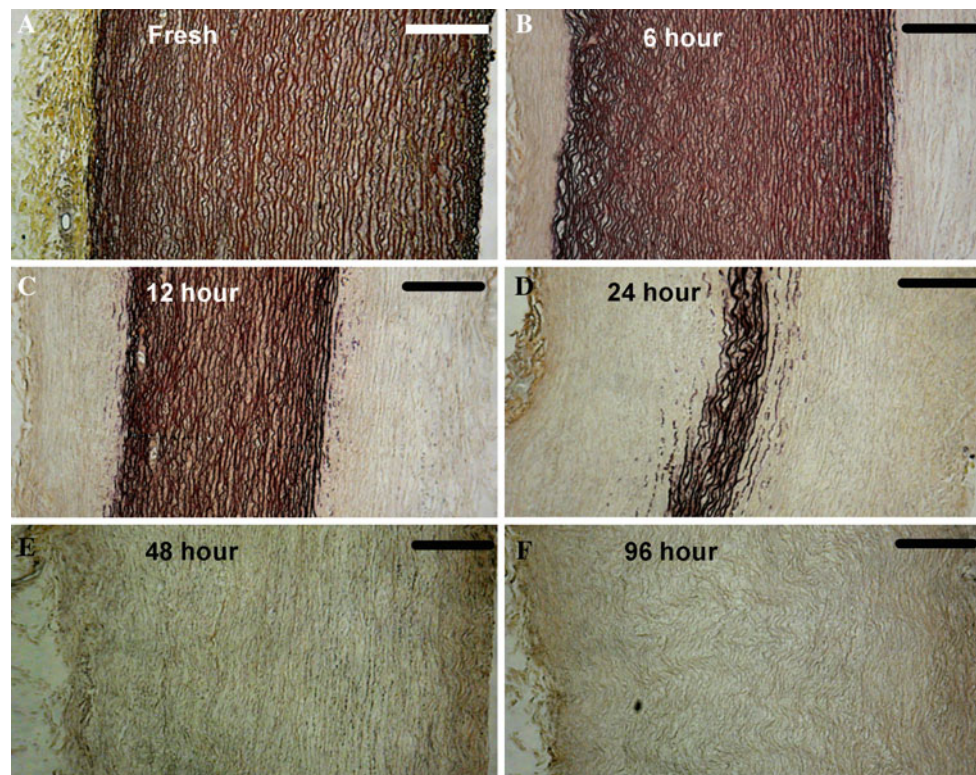


Fig. 4 Histology images of the cross-section of arteries with Movat's Pentachrome stain. The arteries are cut along the *circumferential* direction, and the adventitial side is on the *left* for all six images. Collagen fibers (*yellow*), smooth muscle cells (*red*), ground substance (*blue*),

nuclei/elastic fibers (*purple to black*). Scale bar is 200 μm . Images **a** through **f** show the fresh tissue and samples and after treating with elastase for 6, 12, 24, 48, and 96 h

have a stiff initial slope, a softer middle region and finally the increased slope at higher stresses (Fig. 7a). S-shaped behavior is commonly found in tensile tests of various elastomers (Cheng et al. 2011; Kanyanta and Ivankovic 2010; Lee et al. 2009). Elastomers, such as polyurethanes, are linear segmented copolymer chains and have a structure that consists of loosely coiled domains of polyesters and stiff domains of urethane linkages (Kanyanta and Ivankovic 2010; Oprea and Vlad 2006). At low stresses, the material as a whole is stiff because the load is not high enough to untangle the coiled polyester domains. However, at some threshold stress, the coiled domains will untangle/slip past each other, which leads to large displacements with minimal increase in stress. Once the coiled domains have been straightened out, the material will exhibit strain stiffening as the straightened polyester and stiff domains now bear the load (Lee et al. 2009; Cheng et al. 2011). Our histology studies show that between the digested and undigested regions the ECM in some areas seems undisturbed (highlighted in green) while in other areas, the interconnecting elastic fibers and SMCs are removed (Fig. 7b). Areas affected by the enzyme that have lost the SMCs and interconnecting structure become regions of loose and coiled elastin fibers, while the undigested

regions should be relatively stiff since they retained the original ECM network. We suspect that the cause of the elastomer-like behavior is that the digestion process results in the elastin network having a structure that closely resembles an elastomer. In a previous study of inflation testing on dog carotid arteries, S-shaped behavior occurs in the circumferential direction of the tissue and this is attributed to the waviness of the elastic lamellae in the circumferential direction (Dobrin and Canfield 1984). In our study, the S-shaped behavior is evident in both longitudinal and circumferential directions (Fig. 7a) and so the original structure of the elastic lamellae is not a likely cause for the elastomer-like behavior.

The third stage of the stress versus strain curves is the extensible-but-stiff phase, characterized by a hyperelastic behavior with a very low initial slope and rapid change to a high slope. Based on the histology images and elastin assays, at 24 h, there is limited elastin left in the arterial tissue and this can explain the very low initial slope (Cox 1978; Lacolley et al. 2002). There is a large initial stretch because a small amount of elastin is still present and supporting the initial loading. The high slope in the stress versus strain curves occurs when the collagen fibers have been recruited to support the load. As seen in Fig. 6 (curves

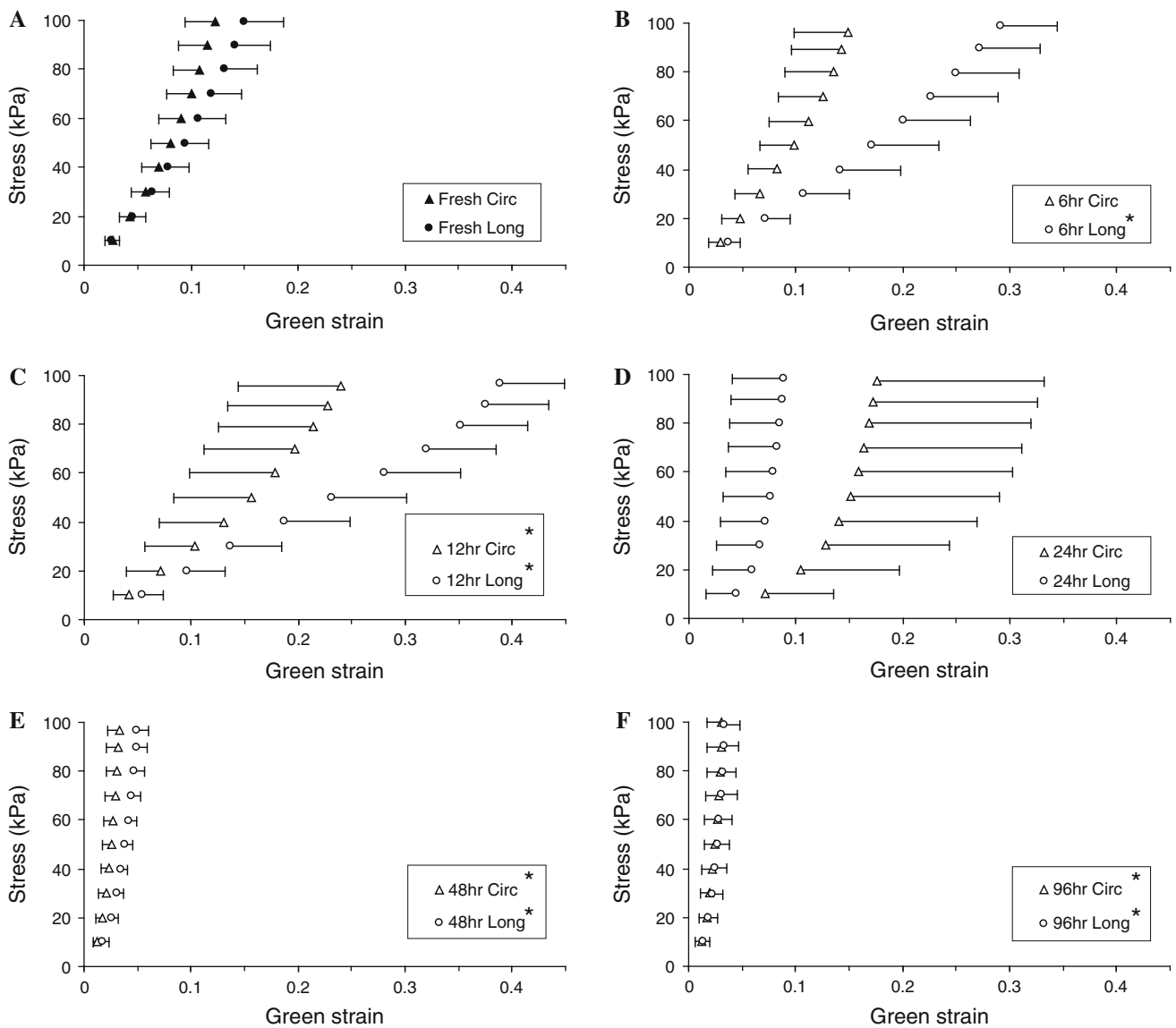


Fig. 5 Averaged Cauchy stress versus Green strain curves. Images **a** through **f** show the fresh tissue ($n = 60$) and samples after treating with elastase for 6, 12, 24, 48, and 96 h ($n = 12$). One-sided *error bars* of

a standard deviation (SD) are shown for the *longitudinal* and *circumferential* directions. * $P < 0.05$ when compared to strains from the corresponding stresses in the fresh condition

labeled ES (a) and ES (b)), the strain at which the curve shifts from low slope to high slope can vary greatly from sample to sample. This is possibly due to sample-to-sample variation such as in artery thickness, as certain arteries at 24 h might be closer to the fourth stage of mechanical behavior. Since digestion occurs from the exterior to interior, thinner samples progress faster toward the collagen-scaffold behavior, which leads to collagen recruitment at lower strains (Intengan et al. 1999). We expect arteries change from the elastomer-like stage into behavior that resembles the ES (a) curve of Fig. 6 because the remaining elastin should still bear the initial load. As the elastin is further degraded, the collagen fibers

are recruited earlier so the shift to a stiff slope is expected to occur to a lower strain (more like ES (b) curve in Fig. 6).

After 48 and 96 h of elastase digestion, there is a complete removal of elastin and the arteries have a collagen-scaffold behavior characterized by a very high slope shortly after the onset of loading. The mechanical behavior measured in this experiment after 48 and 96 h is very similar to those measured in studies of porous collagen scaffolds created from porcine aorta for tissue engineering (Lu et al. 2004). Our biochemical assays and histological studies show minimal elastin left in the tissues at these time points, which explains the lack of the initial soft region because the collagen fibers are the only

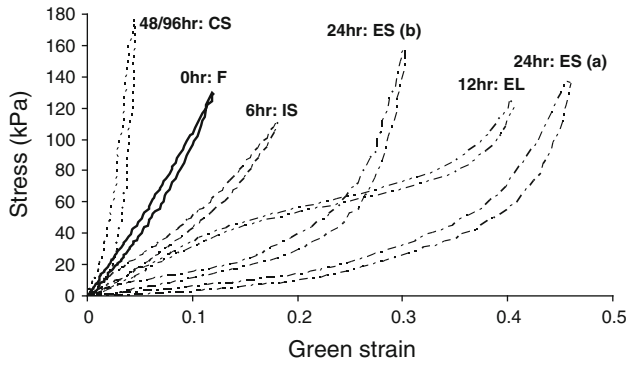


Fig. 6 Representative Cauchy stress versus Green strain curves showing the progression of the mechanical properties through four major stages due to elastin degradation: initial-softening (IS), elastomer-like (EL), extensible-but-stiff (ES), and collagen-scaffold (CS) behavior. Note only the longitudinal direction is shown

component left supporting the load. The reason why the 96 h samples appear isotropic (Fig. 5f) might be due to the fact that the size changes of the sample in the longitudinal and circumferential directions due to elastase digestion were not included. Previously, we have mentioned that the size of the

samples increases due to the elastase digestion (Fig. 1) and because of this, digested samples have “initial stretches”. The amount of initial stretch in the tissue increases with longer digestion times and affects the starting point of the stress versus strain curves. The initial stretches in the longitudinal direction at 96 h are significantly greater than the initial stretches in the circumferential direction (1.395 ± 0.058 vs. 1.326 ± 0.092 , $P = 0.037$). In Fig. 8a, b, these initial stretches due to elastase digestion are included in the Green strain calculations. As shown the Fig. 8b, the tissue samples are still likely anisotropic after 96 h of elastase treatment but appear isotropic if the initial stretch is excluded. It is noted the initial stretch of the longitudinal and circumferential directions for the other time points (6, 12, 24, 48 h) are not significantly different ($P = 0.53$, $P = 0.58$, $P = 0.86$, $P = 0.82$, respectively).

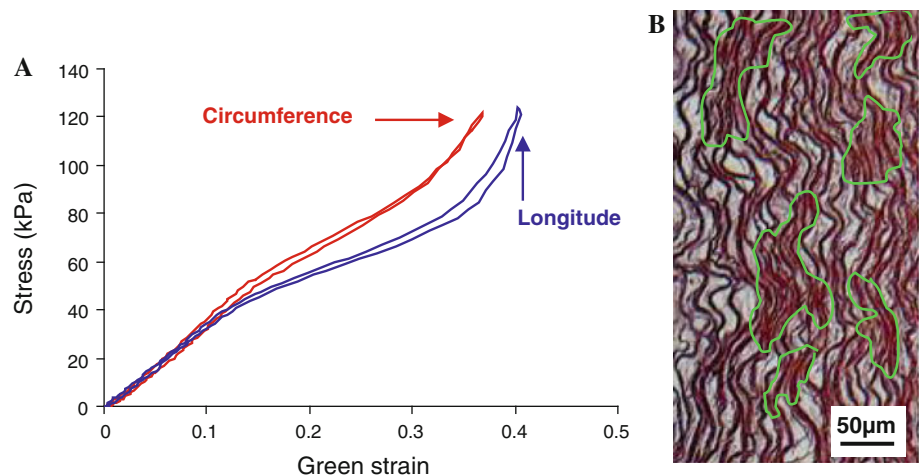
The initial-softening, extensible-but-stiff, and collagen-scaffold stages are expected changes as a result of the elastase digestion however, the elastomer-like stage however has not been reported before. Studies on rubber have shown the presence of an elastic instability such that when a rubber tube is inflated past a certain limit point a local dilation can form

Table 1 The changes in the frequencies of fresh (F), initial-softening (IS), elastomer-like (EL), extensible-but-stiff (ES), and collagen-scaffold (CS) stages with elastin degradation

Stage →	Longitude					Circumference				
	F	IS	EL	ES	CS	F	IS	EL	ES	CS
<i>Digestion time</i>										
0 h	60	–	–	–	–	60	–	–	–	–
6 h	–	4	8	–	–	6	4	2	–	–
12 h	–	–	10	2	–	–	5	7	–	–
24 h	–	–	–	6	6	–	–	–	8	4
48 h	–	–	–	–	12	–	–	–	1	11
96 h	–	–	–	–	12	–	–	–	–	12

The 0h time point corresponds to the tests of the fresh arteries. All arteries were tested at the 0h condition ($n = 60$), and then 12 arteries were tested at each of the digestion time points ($n = 12$)

Fig. 7 a Cauchy stress versus Green strain curves from a sample after 12 h of elastase digestion demonstrating elastomer-like behavior and **b** Movat’s pentachrome stain showing that the digestion process results in the formation of an ECM structure that closely resembles an elastomer with some areas undisturbed (highlighted in green) while in other areas the interconnecting elastic fibers and SMCs were removed. Scale bar is 50 μm



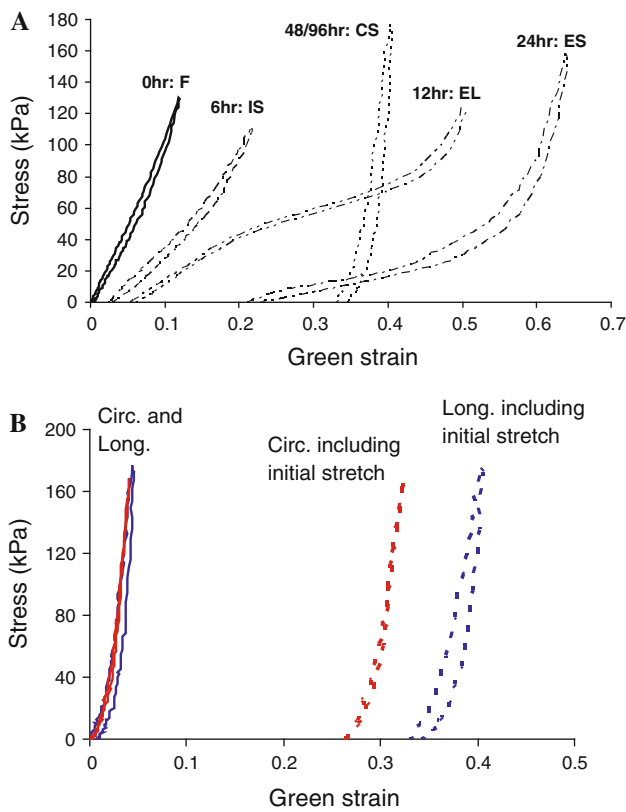


Fig. 8 **a** Cauchy stress versus Green strain curves of the data in Fig. 6 but including the initial stretches due to elastin degradation. **b** Cauchy stress versus Green strain curves of an artery after 96 h digestion with (dotted lines) and without (solid lines) the initial stretches included

(Gent 2005; Bogen and McMahon 1979). This principle of an elastic instability has been suggested as a reason for aneurysm formation (Akkas 1990). Other studies have used simulations to show that limit point instabilities are not the cause of intracranial saccular aneurysms and instead the formation and growth of aneurysms are due to the arterial remodeling (Kyriacou and Humphrey 1996; Taylor and Humphrey 2009). Our results indicate that elastin degradation during the remodeling process may form an elastomer-like structure in the artery, which could contribute to the rapid increase in diameter.

The greater initial stretches in the longitudinal than in the circumferential direction after 96 h of elastase digestion indicates some structural difference in the two directions. The anisotropy of arterial tissue is mainly due to the alignment of families of collagen fibers at a certain angle from the circumferential direction (Dahl et al. 2007). The application of elastase also results in the loss of SMCs and the removal of cells has been shown to reduce collagen fiber crimping in rabbit carotid arteries (Williams et al. 2009). It seems possible that with less fibers oriented in the longitudinal direction, when the fibers uncrimp due to loss of the elastin/SMCs, this leads to the longitudinal direction having a large initial

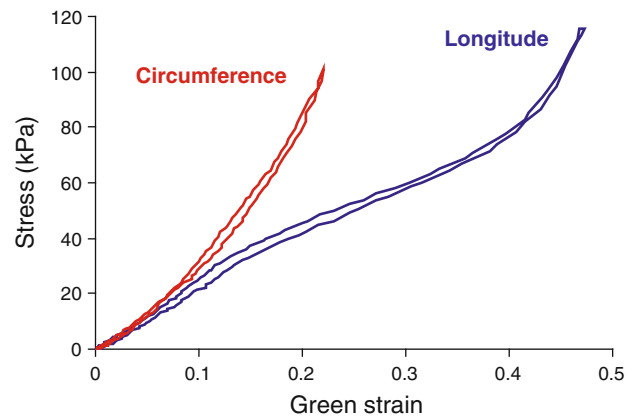


Fig. 9 Cauchy stress versus Green strain curves of an artery after 12 h digestion, showing the longitudinal direction is in the elastomer-like stage while the circumferential direction is in the initial-softening stage

stretch. With the presence of more collagen fiber bundles in the circumferential direction, the uncrimping effect may have been reduced as there is more structure remaining to support the tissue shape.

In general, it appears as though the circumferential direction progresses through the four stages of mechanical behavior more slowly than the longitudinal direction (Table 1). As an example, the circumferential direction is still in the initial-softening stage while the longitudinal direction has already has elastomer-like behavior after 12 h of digestion in the example artery (Fig. 9). The cause of this different rate of progression may be due to the different structure of the elastic lamellae in the two directions. In the circumferential direction, the lamellae are very wavy and corrugated while in the longitudinal direction, the lamellae sheets are fairly flat (Arribas et al. 2006; Clark and Glagov 1985). Stretched elastin fibers are found to be more susceptible to degradation during elastase digestion processes (Jesudason et al. 2007), and this could have led to a faster disruption of the elastin in the longitudinal direction. Studies have shown the corrugated structure of the elastic lamellae in the circumferential direction of rabbit abdominal arteries are not fully straightened until ~80 mmHg (Wolinsky and Glagov 1964). Our samples are digested in elastase solutions without any load, so the waviness of the elastin structure in the circumferential direction could also have delayed the disruption of elastin through a shielding process. The difference in progression of the circumference and longitude also explains the flip in anisotropy seen after 24 h of digestion (Fig. 5d). It is possible that the longitudinal direction is closer to reaching the collagen-scaffold stage and so the initial distensibility is smaller after 24 h. In contrast, the circumferential direction is most likely still within the extensible-but-stiff stage and so the initial distensibility is larger causing the switch in anisotropy of the tissue.

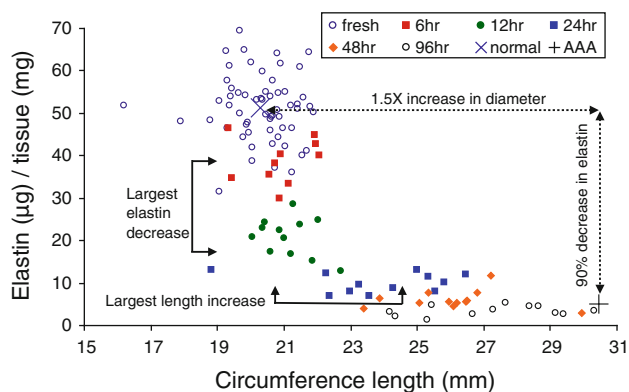


Fig. 10 Elastin content, expressed as μg of elastin per mg of wet tissue weight, versus circumference length at fresh conditions (0h, $n = 60$) and after treating with elastase for 6, 12, 24, 48, and 96 h ($n = 12$). The arrows indicating the $1.5\times$ diameter increase and $\sim 90\%$ elastin decrease are shown to describe the beginning and final tissue states studied in previous literature of AAA

It is generally accepted that AAAs are characterized by a $1.5\times$ increase in diameter and have about a 90% decrease in elastin content (Humphrey and Taylor 2008). These values were measured from non-aneurysmal and aneurysm aortic tissue that had been harvested during preemptive repair surgery (Carmo et al. 2002). However, aneurysm tissue that is harvested to avoid rupture will be already dilated and at the end point of the structural changes that occur as a result of the disease. Our study shows the elastomer-like behavior appeared around 12 h of digestion in elastase. This is also when the greatest decrease in elastin content (occurs between 6 and 12 h) and the greatest increase in circumference length (happens between 12 and 24 h) occurred (Fig. 10). Following a hoop stress estimation based on results from Ohashi et al. (2009), the estimated stresses in porcine descending thoracic arteries ranges between 98 and 180 kPa for diastolic and systolic pressures of 110–170 mmHg, respectively. The elastomer-like behavior for some samples (Figs. 7a and 9) occurs around a Cauchy stress of around 85 kPa, that is, near the stresses experienced during diastole. Note that the stress levels at which the elastomer-like characteristics appear seemed to depend on not only digestion time but also sample thickness. Because our protocol used fixed digestion times, the elastomer-like behavior was evident at various stress levels and thus the change in mechanical properties from being J-shaped to S-shaped could be physiologically relevant and play some role in artery dilation.

In the present study, although stress was reported, we would like to mention the layers of the arterial wall may not bear equal amounts of load and so accurate stress calculations can be compromised. Our histology studies showed that the tissue degradation was occurring unevenly through the thickness. We often have a central band of unaffected layers sandwiched between two bands of collagen layers (where the

elastin had been removed) and these layers of the arterial wall may bear different amounts of load. In addition, due to the creation of the loose and gel-like collagen layer with elastin degradation, the thickness measurement can vary greatly based on the amount of hydration. This can lead to uncertainty in the thickness measurement and further affect the reported stresses.

5 Limitations

There are several limitations in this study and improvements to the digestion and structural analysis methods could give more information about the formation of an elastomer-like structure in arteries. Here, we studied porcine aortas, which differ from human both in structure and pressure ranges (Holzapfel et al. 2005; Ohashi et al. 2009; Vande Geest et al. 2006). Future experiments would benefit from higher tensions to reach stresses experienced during systole. Collagen remodeling and increase of cross-linking of collagen, which does not occur in our study, can lead to collagen recruitment at lower strains (Intengan et al. 1999) and may reduce the elastomer-like behavior. Intima thickening in aneurysm may also compromise the structural/mechanical changes due to elastin degradation. The thickness of the porcine aortas in our study leads to an uneven digestion of the arteries, which is not what occurs normally in aneurysm formation. Using thinner arteries from rats and rabbits, other chemical degradation studies of aneurysm tissue are able to degrade the media more evenly through the entire artery thickness (Guo et al. 2011; Stanley et al. 1975). Another aspect for further investigation is digesting the tissues under physiologic strains. As mentioned earlier, stretched elastin networks are found to be more susceptible to elastase degradation (Jesudason et al. 2007). The sandpaper tab attachment method is different from the conventional hooking method in biaxial tensile testing and may lead to stress concentrations in the corners of the tissue (Sun et al. 2005). Although not shown here, our early validation studies found minimal differences in characterizing the overall tissue behavior between the two methods. Finally, future studies of the artery structure such as examining the collagen and elastin fiber orientation with three-dimensional microscopy will help understand the transition in mechanical properties between healthy and elastin-depleted/dilated arteries.

6 Conclusions

This study intends to determine a relationship between the mechanical properties and the structural/biochemical composition of an artery and give possible insights into the formation of aneurysm. While previous studies have

generally looked at healthy versus already dilated/ruptured tissue, this study investigates the gradual changes in mechanical properties with a mild elastase treatment. Our results show that digestion of elastin in the artery leads to artery dilation in the absence of loading. Four distinct mechanical stages are identified in the digested arteries. The initial-softening, extensible-but-stiff, and collagen-scaffold-like stage are explainable with the changes in elastin measured by the assays and histology techniques. The more interesting elastomer-like stage happens when elastin degradation and increase in circumferential length occur most rapidly. This elastomer-like stage, which may occur during the transition between healthy and dilated tissue states, has not been reported by previous experimental studies of aortic aneurysm. However, the behavior during this transition could be important for artery dilation as the artery has the potential to exhibit large stretches with a minimal increase in pressure. Finally, the circumferential and longitudinal directions of the artery progress through the four stages at different times due to the different organization of elastin in the two directions. Future studies with other digestion solutions under physiologic stresses as well as improved methods of assessing structural changes would make a more complete assessment of the relationship between the mechanical integrity and the microstructure/biochemical composition of arteries.

Acknowledgments This work was supported by a grant from the NIH (HL098028). The authors would like to thank David Zurakowski for discussions on the statistical analysis.

References

- Akkas N (1990) Aneurysm as a biomechanical instability problem. In: Moore F (ed) *Biomechanical transport processes*. Plenum Press, New York, pp 303–311
- Arbustini E, Morbini P, D'Armini AM, Repetto A, Minzioni G, Piovella F, Viganò M, Tavazzi L (2002) Plaque composition in plexogenic and thromboembolic pulmonary hypertension: the critical role of thrombotic material in pultaceous core formation. *Heart* 88(2):177–182
- Arribas SM, Hinek A, Gonzalez MC (2006) Elastic fibres and vascular structure in hypertension. *Pharmacol Therapeut* 111:771–791
- Bogen DK, McMahon TA (1979) Do cardiac aneurysms blow out. *Biophys J* 27:301–316
- Carmo M, Colombo L, Bruno A, Corsi FRM, Roncoroni L, Cuttin MS, Radice F, Mussini E, Settembrini PG (2002) Alteration of elastin, collagen and their cross-links in abdominal aortic aneurysms. *Eur J Vasc Endovasc Surg* 23:543–549
- Cheng H, Hill PS, Siegwart DJ, Vacanti N, Lytton-Jean AKR, Cho SW, Ye A, Langer R, Anderson DG (2011) A novel family of biodegradable poly(ester amide) elastomers. *Adv Mater* 23:H95–H100
- Clark JM, Glagov S (1985) Transmural organization of the arterial media. The lamellar unit revisited. *Arterioscler Thromb Vasc Biol* 5:19–34
- Cox RH (1978) Passive mechanics and connective tissue composition of canine arteries. *Am J Physiol Heart Circ Physiol* 234:H533–H541
- Dahl SLM, Rhim C, Song YC, Niklason LE (2007) Mechanical properties and compositions of tissue engineered and native arteries. *Ann Biomed Eng* 35(3):348–355
- Dobrin PB (1978) Mechanical properties of arteries. *Physiol Rev* 58(2):397–460
- Dobrin PB, Canfield TR (1984) Elastase, collagenase, and the biaxial elastic properties of dog carotid artery. *Am J Physiol* 247(1 pt 2):H124–H131
- Fonck E, Prod'homme G, Roy S, Augsburg L, Rufenacht DA, Stergiopoulos N (2007) Effect of elastin degradation on carotid wall mechanics as assessed by a constituent-based biomechanical model. *Am J Physiol Heart Circ Physiol* 292:H2754–H2763
- Gasser TC, Gorgulu G, Folkesson M, Swedenborg J (2008) Failure properties of intraluminal thrombus in abdominal aortic aneurysm under static and pulsating mechanical loads. *J Vasc Surg* 48(1):179–188
- Gent AN (2005) Elastic instabilities in rubber. *Int J Nonlinear Mech* 40:165–175
- Gertz SD, Kurgan A, Eisenberg D (1988) Aneurysm of the rabbit common carotid artery induced by periarterial application of calcium chloride in vivo. *J Clin Invest* 81:649–656
- Grashow JS, Yoganathan AP, Sacks MS (2006) Biaxial stress-stretch behavior of the mitral valve anterior leaflet at physiologic strain rates. *Ann Biomed Eng* 34(2):315–325
- Guo DC, Regalado ES, Minn C, Tran-Fadulu V, Coney J, Cao J, Wang M, Yu RK, Estrera AL, Safi HJ, Shete SS, Milewicz DM (2011) Familial thoracic aortic aneurysms and dissections: identification of a novel locus for stable aneurysms with a low risk for progression to aortic dissection. *Circ Cardiovasc Genet* 4:36–42
- Hellenthal FAMVI, Geenen ILA, Teijink JAW, Heeneman S, Schurink GWH (2009) Histological features of human abdominal aortic aneurysm are not related to clinical characteristics. *Cardiovasc Pathol* 18:286–293
- Holzappel GA (2000) *Nonlinear solid mechanics: a continuum approach for engineering*. Wiley, New York
- Holzappel GA, Sommer G, Gasser CT, Regitnig P (2005) Determination of layer-specific mechanical properties of human coronary arteries with nonatherosclerotic intimal thickening and related constitutive modeling. *Am J Physiol Heart Circ Physiol* 289(5):H2048–H2058
- Humphrey JD, Eberth JF, Dye WW, Gleason RL (2009) Fundamental role of axial stress in compensatory adaptations by arteries. *J Biomech* 42(1):1–8
- Humphrey JD, Taylor CA (2008) Intracranial and abdominal aortic aneurysms: similarities, differences, and need for a new class of computational models. *Annu Rev Biomed Eng* 10:221–246
- Intengan HD, Thibault G, Li JS, Schiffrin EL (1999) Resistance artery mechanics, structure, and extracellular components in spontaneously hypertensive rats: Effects of angiotensin receptor antagonism and converting enzyme inhibition. *Circulation* 100:2267–2275
- Isenburg JC, Simionescu DT, Starcher BC, Vyavahare NR (2007) Elastin stabilization for treatment of abdominal aortic aneurysms. *Circulation* 115:1729–1737
- Jesudason R, Black L, Majumdar A, Stone P, Suki B (2007) Differential effects of static and cyclic stretching during elastase digestion on the mechanical properties of extracellular matrices. *J Appl Physiol* 103:803–811
- Kallmes DF, Fujiwara NH, Berr SS, Helm GA, Cloft HJ (2002) Elastase-induced saccular aneurysms in rabbits: a dose-escalation study. *Am J Neuroradiol* 23:295–298
- Kanyanta V, Ivankovic A (2010) Mechanical characterization of polyurethane elastomer for biomedical applications. *J Mech Behav Biomed* 3:51–62

- Kyriacou SK, Humphrey JD (1996) Influence of size, shape and properties on the mechanics of axisymmetric saccular aneurysms. *J Biomech* 29(8):1015–1022
- Lacolley P, Boutouyrie P, Glukhova M, Daniel Lamazier JM, Plouin PF, Bruneval P, Vuong P, Corvol P, Laurent S (2002) Disruption of the elastin gene in adult Williams syndrome is accompanied by a paradoxical reduction in arterial stiffness. *Clin Sci (Lond)* 103(1):21–29
- Lakatta EG, Mitchell JH, Pomerance A, Rowe G (1987) Human aging: changes in structure and functions. *J Am Coll Cardiol* 10:A42–A47
- Lasheras JC (2007) The biomechanics of arterial aneurysms. *Annu Rev Fluid Mech* 39:293–319
- Lee LY, Wu SC, Fu SS, Zeng SY, Leong WS, Tan LP (2009) Biodegradable elastomer for soft tissue engineering. *Eur Polym J* 45:3249–3256
- Liang KY, Zeger S (1986) Longitudinal data analysis using generalized linear models. *Biometrika* 73(1):13–22
- Lu Q, Ganesan K, Simionescu DT, Vyavahare NR (2004) Novel porous aortic elastin and collagen scaffolds for tissue engineering. *Biomaterials* 25:5227–5237
- Martinez-Lemus LA, Hill MA, Meininger GA (2008) The plastic nature of the vascular wall: a continuum of remodeling events contributing to control of arteriolar diameter and structure. *Physiology* 24:45–57
- Matsumoto T, Fukui T, Tanaka T, Ikuta N, Ohashi T, Kumagai K, Akimoto H, Tabayashi K, Sato M (2009) Biaxial tensile properties of thoracic aortic aneurysm tissues. *J Biomech Sci Eng* 4(4):518–530
- Miskolczi L, Guterman L, Flaherty JD, Hopkins NL (1998) Saccular aneurysm induction by elastase digestion of the arterial wall: a new animal model. *Neurosurgery* 43(3):595–600
- Ohashi T, Abe H, Matsumoto T, Sato M (2009) Pipette aspiration technique for the measurement of nonlinear and anisotropic mechanical properties of blood vessel walls under biaxial stretch. *J Biomech* 38:2248–2256
- Oprea S, Vlad S (2006) Polyurethane materials for passive isolation bearings. *J Optoelectron Adv M* 8(2):675–681
- Pistea A, Bakker ENTP, Spaan JAE, VanBavel E (2005) Flow inhibits inward remodeling in cannulated porcine small coronary arteries. *Am J Physiol Heart Circ Physiol* 289:H2632–H2640
- Reddy KG (2004) Age-related cross-linking of collagen is associated with aortic wall matrix stiffness in the pathogenesis of drug-induced diabetes in rats. *Microvasc Res* 68(2):132–142
- Sacks MS (1999) A method for planar biaxial mechanical testing that includes in-plane shear. *J Biomech Eng-T ASME* 121:551–555
- Stanley JC, Rhodes EL, Gewertz BL, Chang CY, Walter JF, Fry WJ (1975) Renal artery aneurysms. *Arch Surg* 110:1327–1333
- Sun W, Sacks MS, Scott MJ (2005) Effects of boundary conditions on the estimation of the planar biaxial mechanical properties of soft tissues. *J Biomech Eng* 127:709–715
- Szczesny SE, Peloquin JM, Cortes DH, Kadlowec JA, Soslowsky LJ, Elliot DM (2012) Biaxial tensile testing and constitutive modeling of human supraspinatus tendon. *J Biomech Eng* 134:0210041–0210049
- Tanaka A, Hasegawa T, Chen Z, Okita Y, Okada K (2009) A novel rat model of abdominal aortic aneurysm using a combination of intraluminal elastase infusion and extraluminal calcium chloride exposure. *J Vasc Surg* 50:1423–1432
- Taylor AJ, Gorman PD, Farb A, Hoopes TG, Virmani R (1999) Long-term coronary vascular response to 32P Beta-particle-emitting stents in a canine model. *Circulation* 100:2366–2372
- Taylor CA, Humphrey JD (2009) Open problems in computational vascular biomechanics: hemodynamics and arterial wall mechanics. *Comput Methods Appl Mech Eng* 198(45–46):3514–3523
- Valdez-Jasso D, Bia D, Zocalo Y, Armentano RL, Haider MA, Olufsen MS (2011) Linear and nonlinear viscoelastic modeling of aorta and carotid pressure-area dynamics under in vivo and ex vivo conditions. *Ann Biomed Eng* 39(5):1438–1456
- Vande Geest JP, Sacks MS, Vorp DA (2006) The effects of aneurysm on the biaxial mechanical behavior of human abdominal aorta. *J Biomech* 39:1324–1334
- Vorp DA, Vande Geest JP (2005) Biomechanical determinants of abdominal aortic aneurysm rupture. *Arterioscler Thromb Vasc Biol* 25:1558–1566
- Williams C, Liao J, Joyce EM, Wang B, Leach JB, Sacks MS, Wong JY (2009) Altered structural and mechanical properties in decellularized rabbit carotid arteries. *Acta Biomater* 5(4):993–1005
- Wolinsky H, Glagov S (1964) Structural basis for the static mechanical properties of the aortic media. *Circ Res* 14:400–413
- Zou Y, Zhang Y (2009) An experimental and theoretical study on the anisotropy of elastin network. *Ann Biomed Eng* 37(8):1572–1583